CHAPTER 2

LITERATURE REVIEW

2.1 Dielectric response of materials [1]

The dielectric behavior is mostly concerned with the induced and orientation polarization under external electric fields. The first static dielectric response was presented by Clausius and Mossotti; after that the Debye's theory of dynamic dielectric response was then developed. Normally, the dielectric response may be static electric field response or time-dependence dielectric response. The dielectric response of many materials has been of interest to scientists and technologists for many years. The phenomena of polarization, dielectric loss, ionic conductivity, breakdown and relaxation have been studied intensely. Among these properties, the high dielectric constant and the low dielectric loss are considered as important properties of dielectric materials. The dielectric constant is directly related to one or more of four basic type of electrical polarization as follows:

1. Electronic polarization: due to the opposite displacement of positive nuclei and negative electron within the same atom. Each atom is composed of heavy nuclei surrounded by negative electron cloud. In the presence of an external field the charge clouds become distorted because the paths of the electrons tend to shift against the direction of the applied field as shown in Figure 2.1.

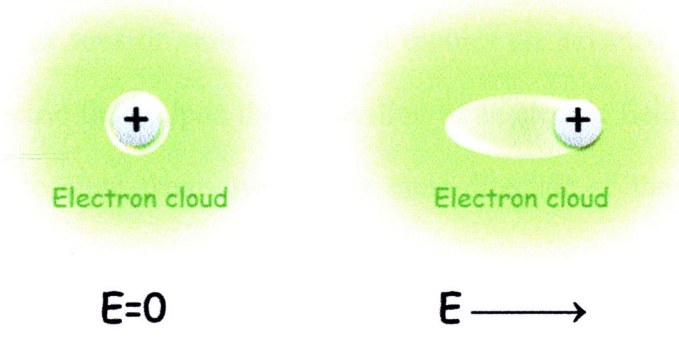

Figure 2. 1 Schematic representation of electronic polarization.

2. Atomic or ionic polarization: due to the relative displacement of positive and negative ions in the substance. Normally, crystals or molecules do not consist of the same kind of atoms, the distribution of charges around an atom in the crystals or molecules leans to positive or negative. Under the external electric field the center positions are changed by the symmetry of the ion displacements, then the polarization arise in the substance as shown in Figure 2.2.

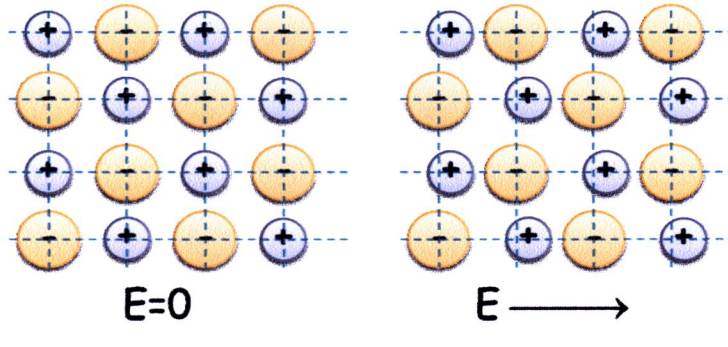

Figure 2. 2 Schematic representation of ionic polarization.

3. Dipolar or orientation polarization: results from the permanent dipoles of complex of complex ions or molecules. Such dipoles are oriented randomly in the absence of an electric field. Upon the application of an electric field, however, these dipoles will tend to align themselves in the same direction of the electric field as illustrated in Figure 2.3.

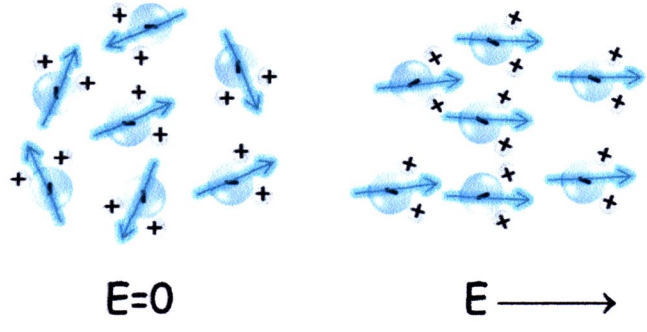

Figure 2. 3 Schematic representation of dipolar polarization.

4. Interface or space charge polarization: due to charge carriers such as mobile and trapped charges that can migrate through the substance. In the absence of an external electric field, the arrangement of these carriers is random and there is no net effect. Upon the application of an electric field, the positive and negative charge carriers will tend to take positions in the direction of the field as shown in Figure 2.4. All of these polarization mechanisms, however, can only operate up to a limiting frequency. As frequency increase, these mechanisms will result in disappearance of polarization as shown in Figure 2.5.

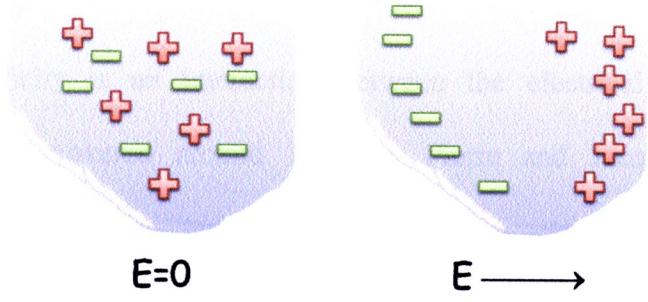

Figure 2. 4 Schematic representations of space charge polarization.

Typically, electronic polarization persists until a frequency of about 10^{16} Hz, ionic polarization until about 10^{13} Hz, while the dispersion for dipolar polarization may lie anywhere within a wide frequency range (i.e.,10^{2}-10^{10} Hz), depending on the material and its temperature. If switching the direction of the field, the direction of the polarization will also switch in order to align with the new field. As a result, time is needed to adjust and called relaxation time.

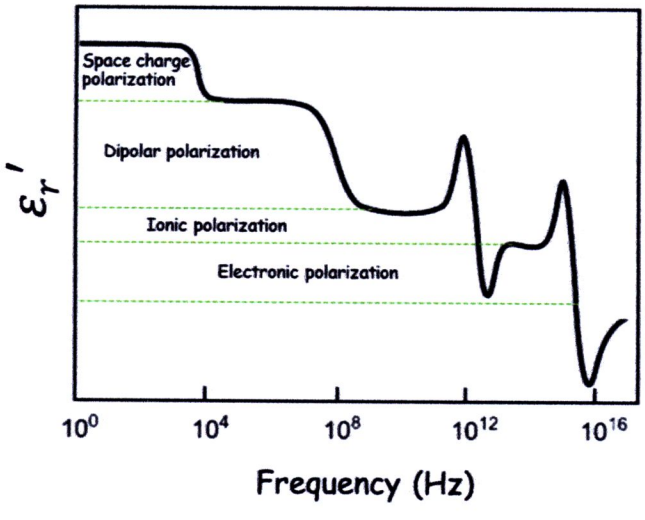

Figure 2. 5 Polarization mechanisms vary with frequency (adapted from Ref.[2]).

2.2 Piezoelectricity

Piezoelectricity is an interaction between the electrical and mechanical systems. It was discovered around 1880 by Pierre and Jacques Curie. They demonstrated an unusual characteristic of certain nonsymmetrical crystalline minerals which are able to develop electrical charges when the mechanical stress is applied, for instance, the deformation of the unit cell which lacks the center of symmetry will induce polarization which is called the direct piezoelectric effect (Figure 2.6 (b)). The mechanical stress generate opposite polarity voltages in the crystal. Conversely, piezoelectric effect is reversible when an electric field is applied; a mechanical strain is then generated (Figure 2.6 (c)).

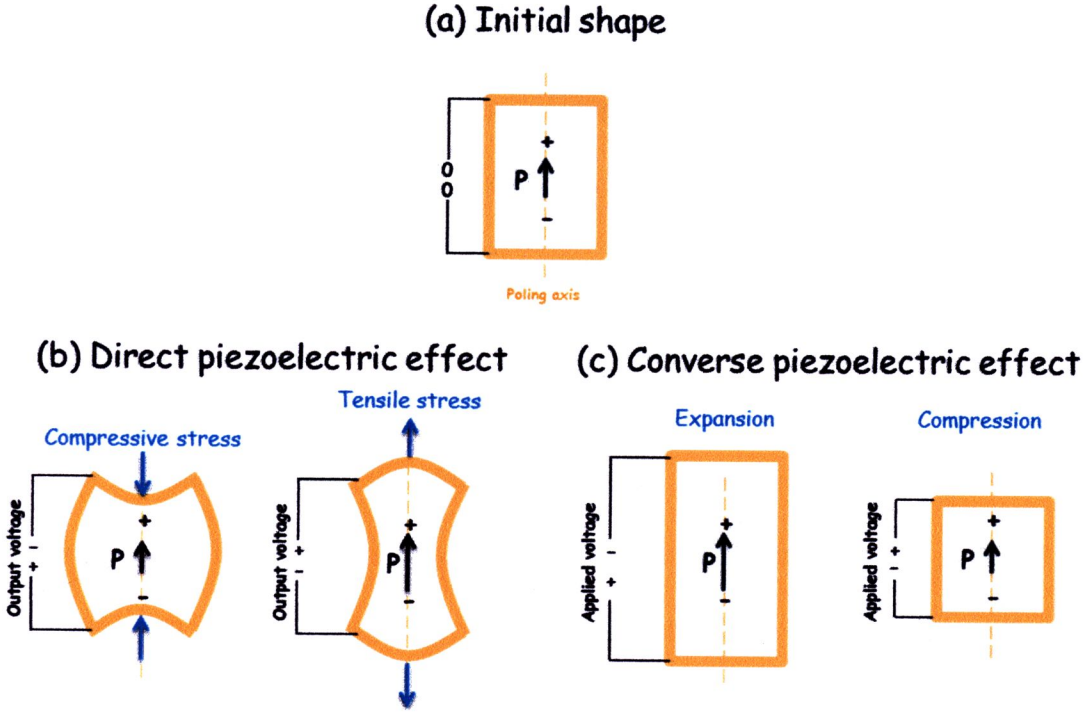

Figure 2. 6 Piezoelectric effects; (a) initial shape (b) direct effect, (c) converse effect.

The direct and converse piezoelectric effects can be expressed in tensor notation as follows [3]:

$$P_i = d_{ijk} \cdot \sigma_{jk} \qquad \text{(direct piezoelectric effect) (2.1)}$$

$$S_{ij} = d_{kij} \cdot E_k \qquad \text{(converse piezoelectric effect) (2.2)}$$

where P_i is the polarization generated along the i-axis in response to the applied stress σ_{jk} and d_{ijk} is the piezoelectric coefficient. For the converse effect, S_{ij} is the strain generated in a particular orientation of the crystal on the application of an electric field E_k along the k-axis. Although the magnitudes of piezoelectric voltages or forces are small, and often require amplification (a typical disc of piezoelectric ceramic will increase or decrease in thickness by only a small fraction of a millimeter, for example) piezoelectric materials have been adapted to an impressive range of applications. The piezoelectric effect is used in sensing applications, such as in force or displacement sensors. The inverse piezoelectric effect is used in actuation applications, such as in motors and devices that precisely control positioning, and in generating sonic and ultrasonic signals.

2.3 Ferroelectricity

A ferroelectric material is defined as being a polar material in the absence of external electric field for which a spontaneous dipole polarization can be switched by the application of an appropriate electric field at certain temperatures [4]. All ferroelectric materials are potentially piezoelectric materials. In addition to reversible spontaneous polarization, the common characteristic of ferroelectrics materials is the

displacement of the polarization hysteresis loops (*P-E*) that can be exhibited at temperatures below the paraelectric-ferroelectric transition temperature as schematically represented Figure 2.7.

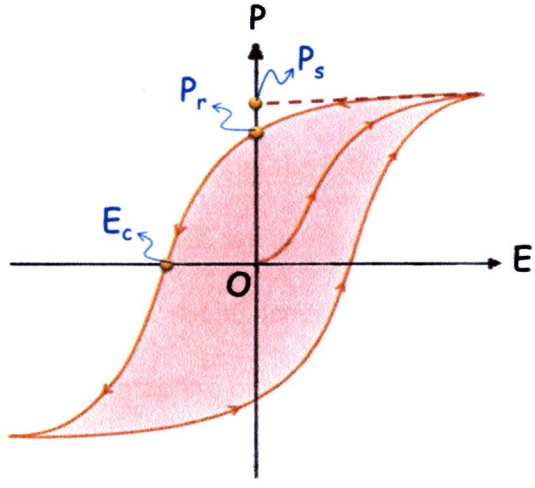

Figure 2. 7 A typical hysteresis loop illustrating the coercive field E_c, spontaneous polarization P_s and remanent polarization P_r (adapted from Ref.[5]).

With increasing electric field, polarization (*P*) in a ferroelectric material increases as a result of switching domain directions and it saturates when all of the domains are aligned in the direction of the electric field (*E*). This state is called saturation polarization (P_s). When the electric field is removed, polarization does not return to zero, but remains at a finite value called remanent polarization (P_r). The electric field that is required to return the polarization to zero is called coercive field (E_c). For most ferroelectrics, there is a critical temperature called Curie temperature (T_c), above which P_s becomes zero then ferroelectricity disappears and paraelectricity (non-polar phase) occurs.

2.4 Phase transition in ferroelectrics and relaxor materials

Phase transition is the transformation of a material from one thermodynamic phase to another, which is accompanied by an abrupt/slow change of certain physical properties of the substance on continuous change of external parameters (temperature, pressure, or some other physical quantities). The crystal structure of many dielectric materials changes with temperature (i.e., they undergo a phase transition). The phase transitions in crystals are due to the change in the forces of interaction between atoms in crystals. This change may produce various new properties in the crystal. The phase transition that produces or alters the spontaneous polarization is called ferroelectric phase transition. By changing temperature or pressure, the atomic arrangements in the crystals may be changed without any change in chemical compositions. The difference in crystal structure on either side of transition temperature (T_c) may be large or small. Usually phase transition in normal ferroelectrics can be classified into two categories:

1. First order transition: A transition in which the chemical potentials of all components in the two phases equal at the transition temperature, but their first derivatives with respect to temperature and pressure, for example, specific enthalpy of transition, specific volume, polarization and structure of a crystal or material are discontinuous at the transition point, as for two dissimilar phases that coexist and that can be transformed into one another by a change in a field variable such as pressure, temperature, magnetic or electric field.

2. Second order transition: In this kind, structure of a crystal and chemical potential undergo a continuous change at the transition point but the second

derivatives with respect to temperature and pressure (i.e. heat capacity, thermal expansion, compressibility) are discontinuous.

Assuming that the ferroelectrics is in a stress-free condition, its elastic Gibb free energy in the one-dimensional (G_1) case can be expressed by a Taylor expansion limiting to sixth-order power term as [6]:

$$G_1(T,D) = \frac{1}{2}\alpha D^2 + \frac{1}{4}\gamma D^4 + \frac{1}{6}\beta D^6 \tag{2.3}$$

where α, γ and β are proportional coefficients, T is temperature and D is dielectric displacement. The electric field (E) and free energy are related by the relation:

$$E = \left(\frac{\partial G_1}{\partial D}\right) = \alpha D + \gamma D^3 + \beta D^5 \tag{2.4}$$

and thus the dielectric permittivity is

$$\frac{1}{\varepsilon} = \left(\frac{\partial E}{\partial D}\right) = \left(\frac{\partial^2 G_1}{\partial D^2}\right) = \alpha + 3\gamma D^2 + 5\beta D^4 > 0 \tag{2.5}$$

The coefficient β is very small and positive in order for G_1 to remain stable as D approaches ∞. For simplicity, γ and β are assumed to be independent of temperature, while α is dependent on temperature in a linear fashion;

$$\alpha = \delta(T - T_0) \tag{2.6}$$

where δ is a positive constant, T_0 is the Curie-Weiss temperature. The sign of α then depends on temperature, and consequently, the sign of γ becomes an important implication that decides the order of phase transition; whether the transition is first-order, γ is negative and γ is positive described the phase transition of second-order. Relation between dielectric displacements, polarization and temperature with and

without applied electric field in the first and second order transition are illustrated in Figure 2.8.

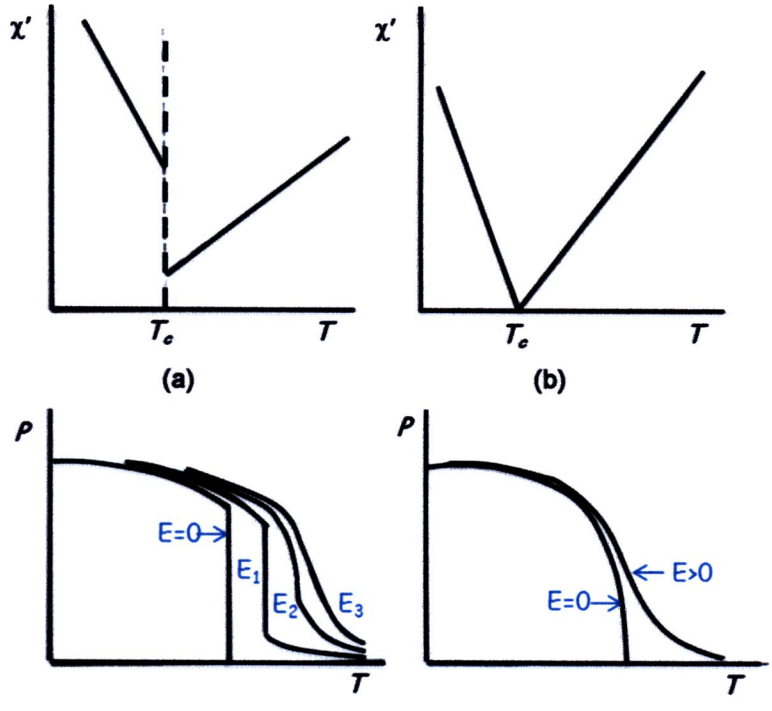

Figure 2. 8 Temperature dependence of reciprocal dielectric constant and polarization in (a) first order transition and (b) second order transition [6].

Ferroelectrics that undergo a transition of the second order, the polarization go smoothly to zero at T_c such that T_0 coincides with T_c. For transition of the first order, the polarization goes to zero discontinuously at T_c and T_0 does not coincide with T_c. Commonly normal ferroelectric materials display a sharp phase transition as shown in Figure 2.9, however, the transition temperature in many macroscopic homogeneous materials is not quite sharply defined. It is mostly smeared over a certain temperature interval known as Curie range, resulting in the gradual change of physical properties.

The width of the Curie region depends on compositional fluctuation and sensitivity of the Curie temperature to composition change. This type of phase transition is generally known as diffuse phase transition (DPT).

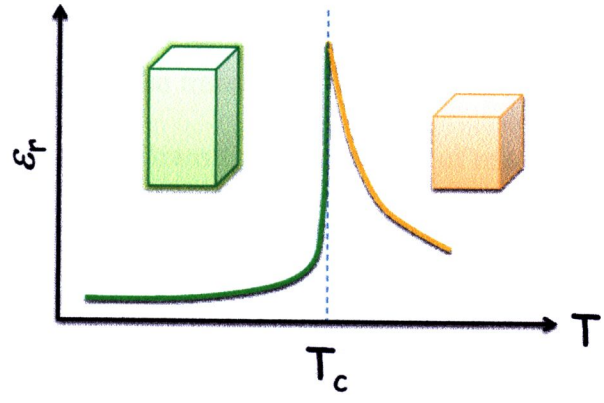

Figure 2. 9 Temperature dependence of relative dielectric constant of ferroelectrics at transition temperature.

Though this phenomenon is observed in several types of materials, the most remarkable example of DPT was found in ferroelectric materials. Ferroelectricity with diffuse phase transitions (FDPT) was first reported in 1951 and their extensive studies were carried out on different systems. FDPT exhibits the broadened maxima in the permittivity-temperature characteristic. The spontaneous polarization of FDPT decreases gradually with rise in temperature. Above the transition temperature, it does not obey the Curie-Weiss behavior. Moreover, the relaxation behavior of dielectric properties is also found in transition region. The diffuseness of the phase transition is assumed to be due to the occurrence of compositional fluctuation and structural fluctuation in a relatively large temperature interval around the transition.

There is a group of materials which does not follow the conditions mentioned above. This group is made up of mixed oxides of perovskite or related structure, and is usually called "relaxor ferroelectrics". The relaxor ferroelectrics may be distinguished from normal ferroelectrics by three distinct properties:

1. Broad diffused phase transition is observed in relaxor ferroelectric over a large temperature range where transition temperature of relaxor ferroelectrics shifts in a large temperature range with frequency along with diffused phase transition.

2. The spontaneous polarization of relaxor ferroelectrics is not lost at T_c of a first or second order transition but decays gradually to zero as shown in Figure 2.10.

3. Most astonishing behavior of relaxor ferroelectrics is that to longer coherence length probing radiations, where samples cooled to very low temperature, show no evidence of optical anisotropy or of the X-ray line splitting.

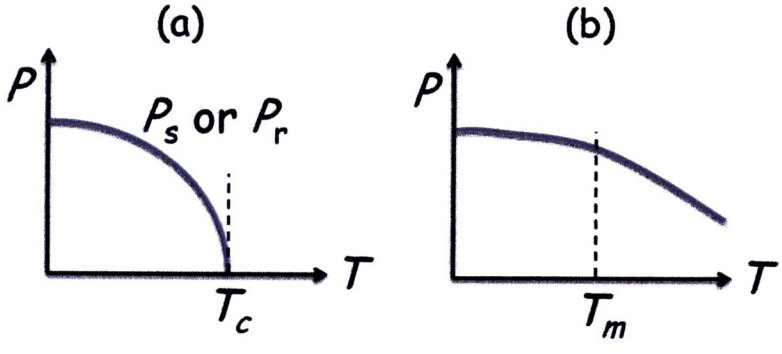

Figure 2. 10 Contrast between the properties of (a) normal FEs and (b) relaxors [6].

The different between diffuse phase transition ferroelectrics (DPT) and relaxor ferroelectrics are shown in Figure 2.11. The phase transition of second-order is

usually encountered in ferroelectric ceramics and above T_c, the temperature dependence of dielectric permittivity can be described by the Curie-Weiss law:

$$\left(\frac{1}{\varepsilon}-\frac{1}{\varepsilon_m}\right) \propto (T-T_m)^{\varphi} \tag{2.7}$$

where ε_m and T_m are the dielectric maximum and the corresponding temperature. When $\varphi = 1$, the dielectric constant follows a normal Curie-Weiss type, showing a sharp transition. When $\varphi = 2$, the transition is a diffused-type.

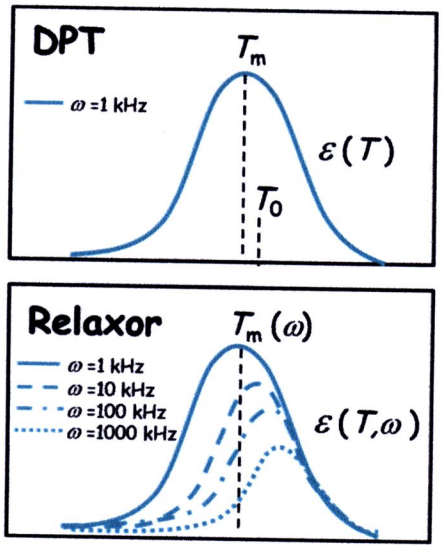

Figure 2. 11 Characteristic properties of DPT and relaxor ferroelectrics.

2.5 Tunable devices [7]

Wireless communication is now accepted as an important part in our everyday life. Many portable compartments have been invented and developed to support growing demand for wireless communication devices. Tunable devices are commonly

used in wireless communication applications such as software defined radio (SDR) application [8] and RF MEMS tunable filters [9].

The basic structure of a typical tunable device is a capacitor as illustrated in Figure 2.12 where a ferroelectric material is placed between two electrodes and biased with an applied voltage. The tuning characteristic of the tunable device is characterized by its ability to change the phase speed v_p of the electromagnetic waves such as radio frequency wave (RF) and microwave propagating through its medium:

$$v_p = \frac{1}{\sqrt{\varepsilon}} \tag{2.8}$$

where ε is the dielectric constant of the tunable element. Due to the extremely high variation in dielectric permittivity under external electric field of ferroelectric materials, the frequency and phase characteristics of its tunable device can be tuned by changing the bias voltage accordingly.

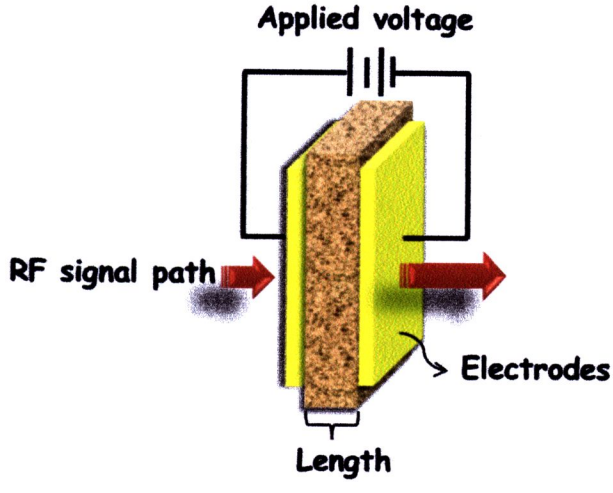

Figure 2. 12 Schematic view of a typical tunable device.

The dependence of dielectric constant on an applied electric field in ferroelectrics can be described through a quantity known as "tunability", defined as:

$$n = \frac{\varepsilon_r(0)}{\varepsilon_r(E)} \tag{2.9}$$

where $\varepsilon_r(0)$ and $\varepsilon_r(E)$ are the dielectric constant at zero field and electric field E, respectively. Practically, the "relative tunability" is used and defined as:

$$n_r = \frac{\varepsilon_r(0) - \varepsilon_r(E)}{\varepsilon_r(0)} \times 100 \tag{2.10}$$

Actually, ferroelectric materials for tunable devices should have high tunability and very low dielectric loss ($\tan\delta$). However the rest of the ferroelectric materials usually possess moderate dielectric loss; therefore enhancing the tunability is normally the main target of many researchers for tunable application's purposes.

2.6 Impedance spectroscopy [10]

Impedance spectroscopy is a material characterization technique which nondestructively studies the response of samples to alternating current (ac) excitations. The technique enables us to evaluate and separate the contribution to the overall electrical properties in frequency domain due to electrode reactions at the electrode/material interface and the migration of charge carriers (ions) through the grains and across the grain boundaries within the specimen sample. In electrical impedance spectroscopy, an alternating current (ac) is driven across a sample, then the impedance (Z^*), which is the relative amplitude between alternating current (*Iac*), voltage (*Vac*), and phase shift (θ) are measured directly at the output. Typically, the

ac impedance is measured for a wide frequency (ω) range from millihertz to megahertz, and information from the sample can be extracted from a model-based analysis. The measured impedance of a sample can be described by the equation below:

$$Z^* = \frac{V_{ac}}{I_{ac}} = |Z(\omega)| < \theta(\omega) \tag{2.11}$$

where $|Z(\omega)|$ is the ratio of amplitude between voltage amplitude and current amplitude, and, $\theta\ (\omega)$ is the phase shift between current and voltage signal. Impedance analysis basically involves the display of the impedance data in different formalism. Different complex formalism is used to characterize different solids and these are interrelated via following relation [11]:

Complex modulus $$M^* = j\omega C_0 Z^* \tag{2.12}$$

Complex permittivity $$\varepsilon^* = (M^*)^{-1} \tag{2.13}$$

Complex impedance $$Z^* = (Y^*)^{-1} \tag{2.14}$$

Complex admittance $$Y^* = j\omega C_0 \varepsilon^* \tag{2.15}$$

where $j = \sqrt{-1}$, ω is the angular frequency ($2\pi f$), C_0 is the vacuum capacitance of the measuring cell and electrodes with an air gap in the place of the sample. The measured impedance data can be plotted [12] in the form of following:

• Bode-Bode plot which consists of real part of the impedance (Z') as function of frequency and imaginary part of the impedance (Z'') as function of frequency.

• A plot which consists of magnitude of impedance ($|Z|$) as function of frequency and phase angle of the impedance (θ) as function of frequency.

• Cole-Cole plot, a plot of real part of the impedance *(Z')* versus imaginary part of the impedance *(Z'')*.

The electrical properties of materials are generally represented by equivalent circuits consisting of a capacitor in parallel with a resistor (Figure 2.13). The capacitor represents the materials' dielectric constant and the resistor represents the materials' conductivity. The dielectric materials are, however, often found to contain both polar and non-polar components. Consequently, their resistances and capacitances also depend on frequency. Due to the simplicity, then the Cole-Cole plots and frequency explicit plots can be used to describe the dielectric behavior and electrical conductivity of the materials. The Figure 2.14 shows the Cole-Cole plot, which is represented by one semicircle, obtained from a sample which consists of the electrode layer in contact with an ideal non-polar dielectric layer which does not have permanent dipole moment. As a result, while an ideal polar dielectric material is purely capacitive and does not have any dipole relaxation time constant, an ideal non-polar dielectric material has a dipole relaxation time constant (τ).

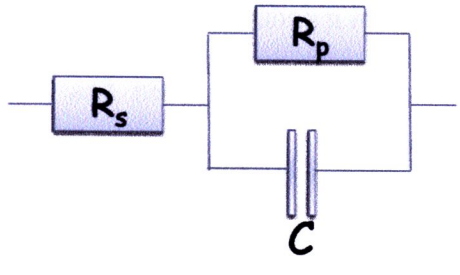

Figure 2. 13 The equivalent circuit model; R_s is electrode's resistance; R_p is material's resistance; C is material's capacitance.

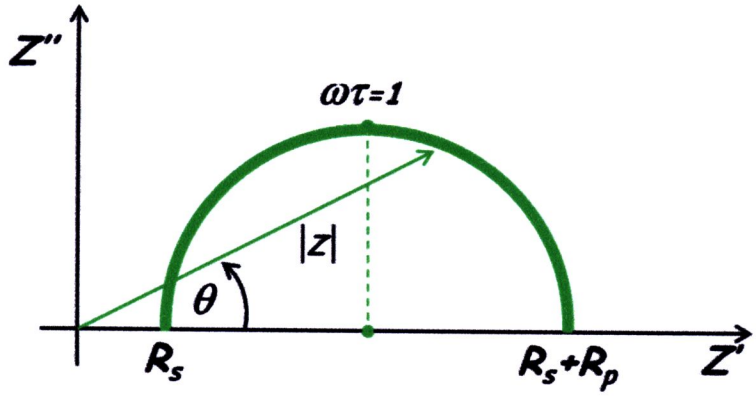

Figure 2. 14 Cole-Cole plot of an ideal non-polar dielectric material.

The magnitude of this dipole relaxation time constant is equal to the product of the resistance and the capacitance of the material ($\tau = RC$).

As has been described earlier, the condition where the samples contain more than one time constant is discussed. To illustrate the properties of Cole-Cole plot of a sample containing more than one time constant, an example is drawn from a sample which consists of three stacked ideal non-polar dielectric layers. The Cole-Cole plot of this three time constants sample contains three semicircles, each associated with the dielectric relaxation time of one particular layer in the sample. The equivalent circuit of this three-time constants sample is shown in Figure 2.15. It consists of three parallel connected capacitor and resistor pairs connected in series. The electrical properties of the first arc at low frequency rang represented the electrode-interface phenomena, the electrical properties of the semicircular arc at intermediate frequency rang represented the grain boundary effects and the electrical properties of the arc at high frequency rang represented the grain interior properties.

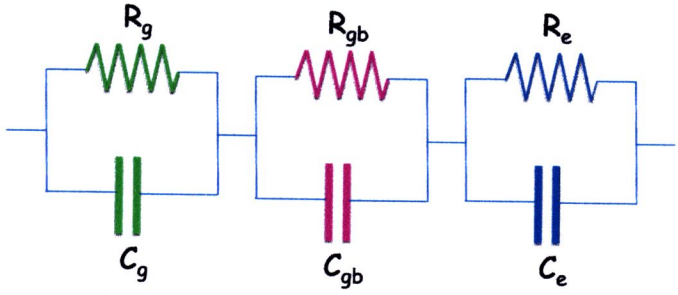

Figure 2. 15 The equivalent circuit of a complex dielectric material; R_g: resistance of grain interior, C_g: capacitance of grain interior, R_{gb} resistance of grain boundary, C_{gb}: capacitance of grain boundary, R_e resistance of electrode, C_e: capacitance of electrode.

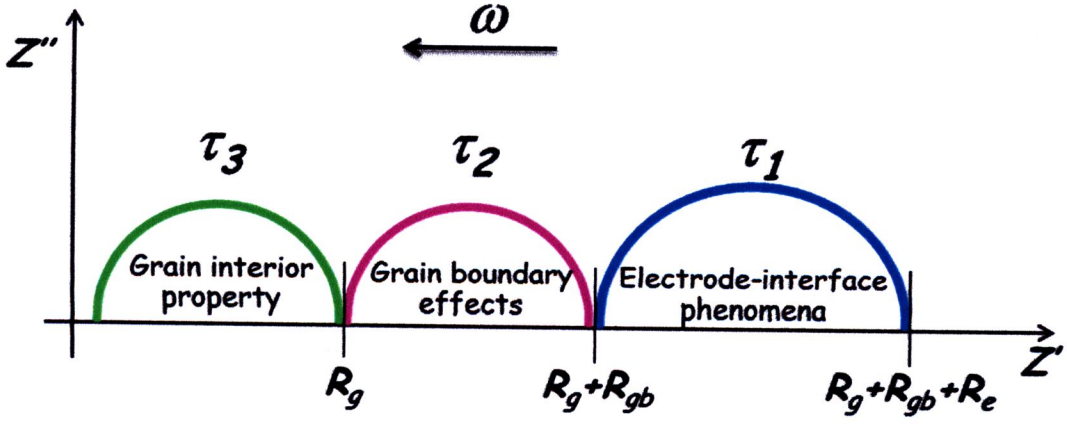

Figure 2. 16 Cole-Cole plot of a complex dielectric material (adapted from Ref.[1]).

The general rule of the semicircles ordering for this three dielectric layer sample is as follows: the semicircle which associated with a layer which has larger time constant value is always observed at the lower frequency of the Cole-Cole plot. For example, the corresponding Cole-Cole plot of a sample which consists of three dielectric layers of different time constants, τ_1, τ_2, τ_3, where $\tau_1 = R_gC_g > \tau_2 = R_{gb}C_{gb} > \tau_3 = R_eC_e$ is translated into an arrangement of semicircles as follows (see Figure 2.16);

the τ_1 semicircle appears at the low frequency range of the Cole-Cole plot, followed by the τ_2 semicircle at mid-frequency range, and, finally by the τ_3 semicircle at the high frequency range.

2.7 Perovskite-oxide type

Perovskite is a group of ferroelectrics which are most commonly studied. Its general chemical formula is ABO_3, where A is lower charged and larger cations (Ca^{2+}, Pb^{2+}, Na^{+}, Ba^{2+}, etc.) placed at the corners of a simple cubic structure, B is smaller and higher charged cations (Zn^{2+}, Nb^{5+}, Ti^{4+}, Mg^{2+}, Zr^{4+}, Co^{2+}, etc.) located at the body centers and O is oxygen atoms designated at the face centers (Figure 2.4). This structure can also be regarded as a set of BO_6 octahedral arranged in a simple cubic pattern and linked together by shared oxygen atoms, with A atoms occupying the spaces in between them. A wide variety of cations can be substituted in the perovskite structure. The relationship below gives the tolerance factor (t)

$$t = \frac{R_A + R_O}{\sqrt{2}(R_B + R_O)} \tag{2.16}$$

where R_A, R_B, and R_O are the ionic radius of large cation, small cation, and anion, respectively. An ideal cubic perovskite structure correspond to when $t = 1$. In practice, most structures having a tolerance factor of between 0.95 and 1.0 are cubic; those with lower values are slightly distorted but non-ferroelectric and those slightly over 1.0 tend to be ferroelectric. On cooling from high temperatures the perovskite structure undergoes single phase transition in some materials like $PbTiO_3$ and multiple phase transitions in some materials ($BaTiO_3$, $NaNbO_3$, etc.). These phase

transitions can be ferroelectric, antiferroelectric or some structural transitions involving non-polar phonons.

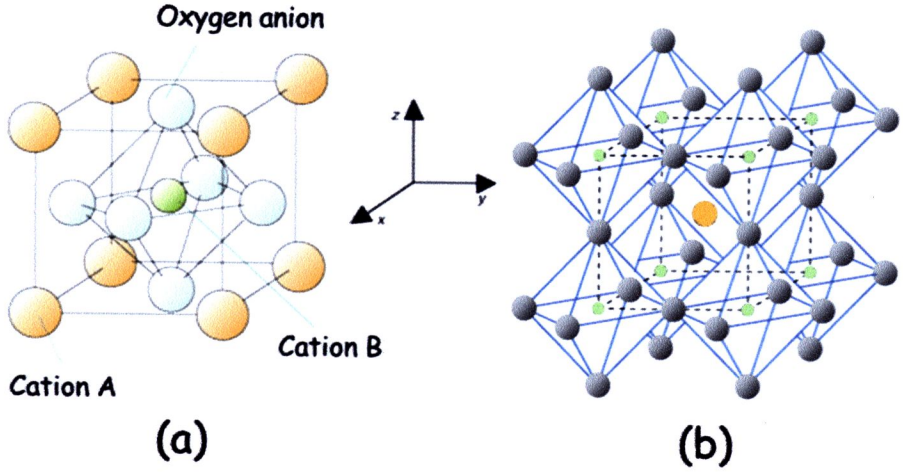

Figure 2. 17 Cubic perovskite structure represented as (a) a unit cell of ABO_3 and (b) network of BO_6 octahedra (adapted from Ref.[13]).

2.8 Barium stannate titanate ceramics: $Ba(Ti_{1-x}Sn_x)O_3$ (BTS)

Barium titanate ($BaTiO_3$) perovskite ceramic is one of the most important electric materials and widely used for capacitors and other electronics devices [14]. It exhibits several ferroelectric phase transitions in the low-temperature range including a tetragonal-cubic transition at around 120°C as shown in Figure 2.18, which causes significant anomaly of the dielectric constant [15]. However, the dielectric constant of pure barium titanate rises sharply with temperature, which is undesirable for practical applications since they are to be used over a wide range of temperature. Therefore, a large number of modified $BaTiO_3$-based ceramics were studied [16-18]. It can be

modified with various solid solutions and additives to raising the temperature range [19, 20].

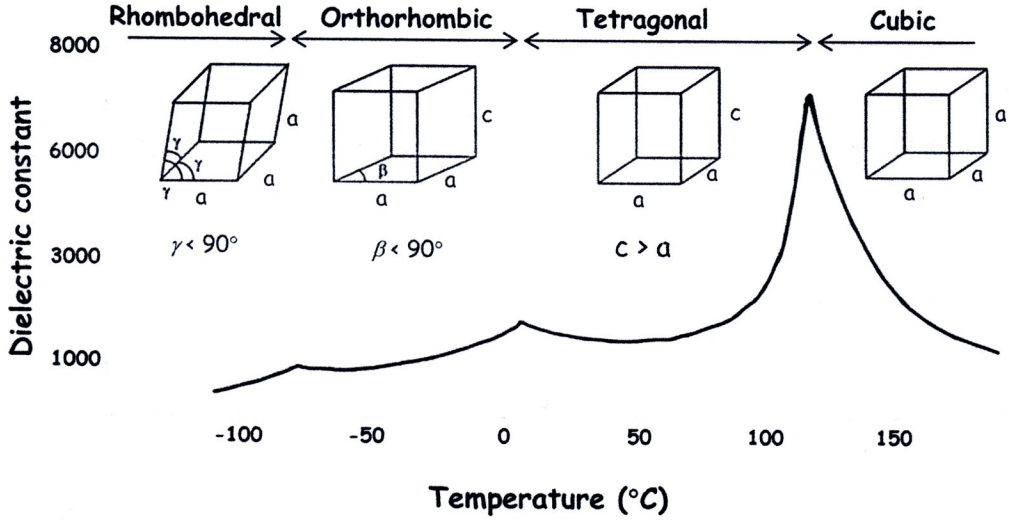

Figure 2. 18 $BaTiO_3$ exhibits dielectric behavior with temperature change (adapted form Ref.[21]).

Barium stannate titanate: $Ba(Ti_{1-x}Sn_x)O_3$ (BTS) is a binary solid solution system. It was firstly investigated in 1970 by Smolensky [22] as a prototype of diffuse phase transition. In 1993, Bao et al. [23] synthesized barium stannate titanate by the method of co-precipitation and added the dopants (Dy_2O_3, Nb_2O_5 and ZnO). They found that value of dielectric constant could reach more than 7000 at room temperature; moreover, it was improved when complex additives were introduced due to an overlapping effect.

In the next few years, Yasuda et al. [24] investigated the pressure-temperature dependence of the dielectric constants at various frequencies in BTS. They obtained

the maximum dielectric constant at x = 0.1 and found the ferroelectric phase changes to the diffuse transition. At the early 2000s, Kajtoch [25] confirmed the previous results by the measurements of a.c. conductivity of BTS solid solution. He concluded that increasing in Sn concentration reaches the value 0.1, the value of dielectric constant increases in the order of 10^3 and the ferroelectric phase (FE)-paraelectric phase (PE) transformation becomes more diffuse, but transition temperature is decreased. Furthermore, when the Sn concentration is higher than 0.1, the BTS has only one ferroelectric transition and no other structural phase transitions.

During 2003-2004, there are many attempts to understand this system. Wang et al. [26] investigated the dielectric characteristics and their tunability with microstructures and diffused phase transition temperature. It was observed that the tunability increases with increasing an electric field, while it drops sharply when the temperature is above T_m. With increasing Sn content, the tunability at room temperature drops due to T_m decreasing.

A few years later, the processing route of BTS ceramics were optimized in full composition range by Wei et al.[27]. They suggested that the optimized sintering temperature is in the vicinity of 1300°C in $Ba(Ti_{0.4}Sn_{0.6})O_3$. The dielectric constant decreases with increasing Sn content. The phase transition becomes diffused when tin content is larger than 0.1, and relaxation behavior can be observed in the sample with the Sn content equal to 0.3.

Recently, Shvartsman et al.[28] investigated the dielectric relaxation of BTS ceramics. Their results suggested that the composition with $0.175 \leq x \leq 0.25$ show coexistence of both ferroelectric and relaxor characteristics.

2.9 References

[1] R.N.P. Choudhary, S.K. Patri, Dielectric materials : introduction, research and applications, Nova Science Publishers, New York, 2009.

[2] R.D. Levi, R. Clive, Solid solution trends that impact electrical design of submicron layers in dielectric capacitors, in, Pennsylvania State University, University Park, 2009, pp. 274.

[3] K.K. Rajan, Growth and Property Characterization of Relaxor Ferroelectric PZN-PT Single Crystals, in: Mechanical Engineering, National University of Singapore, Singapore, 2007.

[4] F.C. Kartawidjaja, Heterolayered $Pb(Zr_xTi_{1-x})O_3$ Thin Films, in: Materials Science and Engineering, National University of Singapore, Singapore, 2009.

[5] http://www.daviddarling.info/encyclopedia/H/hysteresis_loop.html, in.

[6] T. Mitsui, I. Tatsuzaki, E. Nakamura, An introduction to the physics of ferroelectrics, : Gordon and Breach Science Publishers, New York, 1976.

[7] D.T. Manh, Microstructure, Tunable and Pyroelectric Properties of Laser-Ablated Ba $(Zr_{0.25}Ti_{0.75})O_3$ Thin Films, in: Mechanical Engineering, National University of Singapore, Singapore, 2009.

[8] G.L.N. Rao, K.V. Saravanan, K.C.J. Raju, Ferroelectric thin film based tunable devices for software defined radio application, in: TENCON 2008 - 2008 IEEE Region 10 Conference, 2008, pp. 1-5.

[9] Y. Zhu, M.R. Yuce, S. Moheimani, A low-loss MEMS tunable capacitor with movable dielectric, in: Sensors, 2009 IEEE, 2009, pp. 651-654.

[10] P.G.I. Suryacandra, Adaptation and application of a State-Of-The-Art impedance analyzer for characterization of silicon P-I-N diodes, in: Mechanical Engineering, National University of Singapore, Singapore, 2011.

[11] I.M. Hodge, M.D. Ingram, A.R. West, Impedance and modulus spectroscopy of polycrystalline solid electrolytes, Journal of Electroanalytical Chemistry, 74 (1976) 125-143.

[12] J.R. Macdonald, Impedance spectroscopy : emphasizing solid materials and systems, : Wiley, New York, 1987.

[13] T. Imai, M. Sasaura, K. Nakamura, K. Fujiura, Crystal growth and electro-optic properties of $KTa_{1-x}Nb_xO_3$, NTT Technical Reveiw, 5 (2007) 1-8.

[14] A.J. Moulson, J.M. Herbert, Electroceramics : materials, properties, applications, Chapman and Hall, New York, 1990.

[15] V. Petrovsky, T. Petrovsky, S. Kamlapurkar, F. Dogan, Dielectric constant of barium titanate powders near curie temperature, Journal of the American Ceramic Society, 91 (2008) 3590-3592.

[16] Z. Yu, C. Ang, R. Guo, A.S. Bhalla, Ferroelectric-relaxor behavior of $Ba(Ti_{0.7}Zr_{0.3})O_3$ ceramics, Journal of Applied Physics, 92 (2002) 2655-2657.

[17] S.G. Lu, Z.K. Xu, H. Chen, Tunability and relaxor properties of ferroelectric barium stannate titanate ceramics, Applied Physics Letters, 85 (2004) 5319-5321.

[18] S.G. Lu, Z.K. Xu, Tunability and permittivity-temperature characteristics of highly (100) oriented compositionally graded $(Ba_{0.7}Sr_{0.3})(Sn_xTi_{1-x})O_3$ thin films grown by pulse-laser deposition, Applied Physics Letters, 89 (2006) 152907-152903.

[19] K.H. Ahn, S. Baik, S.S. Kim, Significant suppression of leakage current in $(Ba,Sr)TiO_3$ thin films by Ni or Mn doping, Journal of Applied Physics, 92 (2002) 2651-2654.

[20] P.C. Joshi, M.W. Cole, Mg-doped $Ba_{0.6}Sr_{0.4}TiO_3$ thin films for tunable microwave applications, Applied Physics Letters, 77 (2000) 289-291.

[21] http://www.murata.com/products/capacitor/faq/mlcc/index.html.

[22] G.A. Smolensky, Physical phenomena in ferroelectrics with diffused phase transition, Journal of the Physical Society of Japan, 28, Supplement (1970) 26-37.

[23] M. Bao, W. Li, P. Zhu, Study on the dielectric properties of oxide-doped $Ba(Ti,Sn)O_3$ ceramics prepared from ultrafine powder, Journal of Materials Science, 28 (1993) 6617-6621.

[24] N. Yasuda, H. Ohwa, K. Arai, M. Iwata, Y. Ishibashi, Effect of hydrostatic pressure in barium titanate stannate solid solution $Ba(Ti_{1-x}Sn_x)O_3$, Journal of Materials Science Letters, 16 (1997) 1315-1318.

[25] C. Kajtoch, Electric conductivity of $BaTi_{1-x}Sn_xO_3$ solid solution, Materials Science and Engineering: B, 64 (1999) 25-28.

[27] X. Wei, X. Yao, Preparation, structure and dielectric property of barium stannate titanate ceramics, Materials Science and Engineering: B, 137 (2007) 184-188.

[28] V.V. Shvartsman, J. Dec, Z.K. Xu, J. Banys, P. Keburis, W. Kleemann, Crossover from ferroelectric to relaxor behavior in BaTi1− x Sn x O3 solid solutions, Phase Transitions, 81 (2008) 1013-1021.